Chapter 3

Electrochemical Scanning Tunneling Microscopy (ECSTM) – From Theory to Future Applications

Ajay Kumar Yagati, Junhong Min and Jeong-Woo Choi

Additional information is available at the end of the chapter

http://dx.doi.org/10.5772/57236

1. Introduction

The development of scanning tunneling microscopy (STM) clearly forms the creation of a new research tool by innovative implementation of scientific and technological knowledge, thereby advancing further in the fundamental science and technology [1,2]. The quantum-mechanical phenomenon of electron tunneling had been known for a long time, but the use of this phenomenon for the imaging of a conductive surface at atomic level was realized only in 1982 when the first STM as built by Binnig et al [3]. STM has a resolution of a few Ångstrom in lateral directions and less than one Ångstrom in the direction perpendicular to the surface [4]. It consists of a scanning tip which images the surface by means of a tunnel current. Hence, the sample needs to be conductive [5]. At present, STM is a powerful tool for analyzing metallic and semiconductor surface. The real-space visualization of surface at atomic scale is one of the most important features [6]. The spatial variation of the tunneling current or the spatial variation of the tip height is converted in to the real space image. The tunneling current decreases exponentially with the increase in tip-sample distance. Thus, at any given location of tip over the sample surface, the electron transfer involves only one atom or few atoms at the tip apex and on the surface closest to them. This makes it possible to visualize the structures with sub-angstrom resolution and to detect atomic scale defects that are not possible with other spectroscopic techniques [7,8]. The STM not only provides the three-dimensional information about the topography of the sample, but it also gives the information about the spectroscopic properties and local variations of work functions. Further, as a nanofabrication tool, STM can be used for atom manipulation, local deposition and imaging of the molecules [9]. Moreover, STM can be used to operate in air, ultra high vacuum (UHV) and in liquid solutions for electrochemistry applications which involves the immersion of the STM probe into the liquid

media and the corresponding electrochemical control (ECSTM) for *in situ* monitoring of redox processes on the sample electrode [10,11]. Having these advantages STM has become most widely accepted analytical measurement system in the current research works.

2. Fundamentals of scanning tunneling microscopy (STM)

2.1. Origin and operation mode:

The scanning tunnelling microscope was developed by Binnig, Rohrer, Gerber and Weibel [12]. Since STM can be used for imaging on at atomic scale level, this belongs to the most powerful experimental techniques of surface science. In STM, a sharp metallic tip is placed very close to the surface and a small bias voltage is applied between the tip and the sample. As a result, a current of electrons (I_T), flows between the electrodes through the vacuum gap. This process is a quantum mechanical phenomenon and is called as "tunnelling" effect [13] shown in Fig. 1. The electrons "tunnel" through this electrically insulating layer, giving rise to a measurable current which displays an exponential dependence on the distance between the two conducting electrodes [14]. The tunneling current flowing between the STM tip and the sample surface through the insulating gap (s) under an applied V_{bias} which can be explained in a simple analytical tunneling expression assuming a 3-dimensional (3D) metal-insulator-probe junction into a one-dimensional metal-insulator-metal contact. The derived equation that relates with the applied V_{bias} with I_{T} and s yields [15]:

$$I_T = I_o \frac{V_{bias}}{s} e^{-k\sqrt{\phi_b S}} \tag{1}$$

It is the exponential dependence of the tunneling current on the distance between the two conductors (STM tip and the underlying surface) that provides the sensitivity of the measured current that can be interpreted as the surface structure. As the equation shows, other factors influence the current as well, such as the electron band structure of the two conductors (φ).

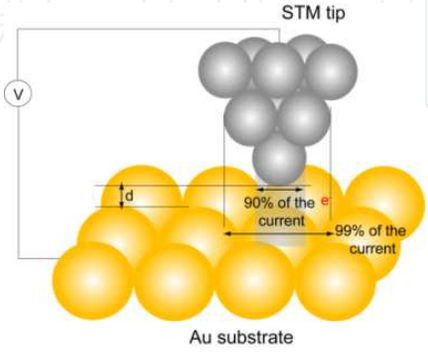

Figure 1. Schematic diagram of scanning tunneling microscopy depicts the tip sample interaction and the tunneling current between the tip and the sample surface.

http://dx.doi.org/10.5772/57236

2.2. Tunnelling methods

2.2.1. General modes of operation

Basically there are two modes in which STM can be operated. The first one being the constant current and the other one is termed as constant height. In the constant current mode, the tip is scanned over the surface at constant tunnel current, and the vertical tip position will be continuously changed to keep the tunnel current as a constant. In ideal conditions, at a homogenous surface constant current refers to constant interval between sample surface and the tip. In this mode, the height control mechanism will adjust the tip to move vertically up and down to keep the tunnel current to a constant value by the feedback voltage [16]. In the constant height mode which most effective for the investigation of atomically smooth surfaces (Z remains *const*). In this mode of operation, the tip moves above the surface at a distance of several Å, and the changes in the tunneling current are recorded as STM image [17]. Scanning may be done either with the feedback system switched off (here no topographic imaging is recorded), or at a speed exceeding the feedback reaction speed (only smooth changes of the surface topography are recorded). This method employs very high scan rates and fast STM images acquisition, allows observing the changes that occur on a surface in a real time.

2.2.2. The electrochemical STM (ECSTM) model

The electrochemical scanning tunneling microscopy (ECSTM) is an extended technique performed along with basic STM measurements for the study of electrode-electrolyte interfaces. Therefore, the same elements as in a standard STM experimental set up can be observed in the ECSTM set-up. The tunneling current flowing between a metallic tip and a conductive sample will be again used to obtain topographical information as well as the electronic structure of a determined electrode surface immersed in the corresponding electrolyte [18,19]. Even though, the fundamentals of both techniques are essentially the same, but two different elements were introduced in a conventional STM set up in order to control as an ECSTM: 1) a three electrode electrochemical cell in which the substrate used as a working electrode, a reference and a counter electrode completed the electrochemical cell. This configuration resembles as a normal three electrode configuration coupled to a potentiostat in which the potential of the working electrode can be controlled with respect to a high-impedance reference electrode, while the current is allowed to flow between the working and the counter electrode. 2) Development of suitable ECSTM probes. In this case, the tip is not an active electrode in the cell, but used only to image the surface morphology, even if it had to be under potential control in order to apply a voltage drop to drive the tunnelling current. The implementation of a liquid STM represented a great breakthrough for the in situ study of surface electrodes [20]. An improvement in the STM has been obtained with the introduction of the bipotentiostat approach, in which both tip and sample potentials are independently controlled with respect to a reference electrode in solution.

3. Electrochemistry in scanning probe microscopy: Basic concepts and applications

The electrochemical scanning tunneling microscope was the first tool for the investigation of solid-liquid interfaces that allowed in situ real space imaging of the underlying electrode surfaces at atomic level. Therefore ECSTM gained much importance and emerged as a prominent tool for the determination of the local surface structure as well as the dynamics of reactions/ processes that takes place at surfaces in an electrolytic environment. Although the fundamentals of both techniques are then essentially the same, but two different elements must be introduced in a conventional STM set up in order to operate as an ECSTM: an electrochemical cell consisting of two working electrodes with bipotentiostat approach and suitable ECSTM probes [21].

3.1. Preparation of reliable probes, tunneling in liquid environments at a bipotentiostat configuration

The general electrochemical experiment which is composed with standard potentiostat, the potential of the working electrode is controlled with respect to a reference electrode by the flow of current through a counter electrode. However, in ECSTM with *in-situ* electrochemical measurements, the same potentiostatic approach is able to control both the potential of the substrate and the potential of the tip that is present in solution with respect to a reference electrode in order to control electrochemical reactions taking place at its surface, which is practically not possible [22,23]. Generally in STM, it is expected that the current enters into the measuring system due to the charge transfer process is mainly due to tunneling current between the tip and the substrate. If the potential of one of these two electrodes is not controlled in the electrochemical cell, then electrochemical charge transfer mechanisms might become significant and contribute to the measured currents which leads to a strong source of noise in the STM control circuit [24,25]. Further, the absence of control on the electrochemical potential of one electrode in an electrochemical cell also gives rise to phase variation in the surface composition of the electrode. In this aspect, with bipotentiostatic approach an independent control on the potential of both the tip and the substrate with respect to a reference electrode in solution is established for the development of the *in-situ* STM.

The main purpose of the potentiostat is to control the potential of the electrode in an electrochemical cell from various impedances connecting to these electrodes. The controller maintains the potential of the reference with respect to the working electrode in such a way that the potential is exactly opposite to the controlled potential, which is free from fluctuations of the impedances [26]. Hence, the bipotentiostat controls the potential of two electrodes with respect to a reference electrode. The ECSTM setup is depicted in Fig. 2. Generally, the tip is virtually grounded and the tunneling current is measured by a high-gain current follower or it is fed to the STM control unit through a preamplifier. In all configurations, the tip and substrate potentials are controlled with respect to a current less reference electrode. Usually, the counter electrode in EC-STM setup is obtained by an Au or Pt wire which has enough stability [27]. Also, a good reference electrode is obtained when a metal is used in electrochemical equili-

http://dx.doi.org/10.5772/57236

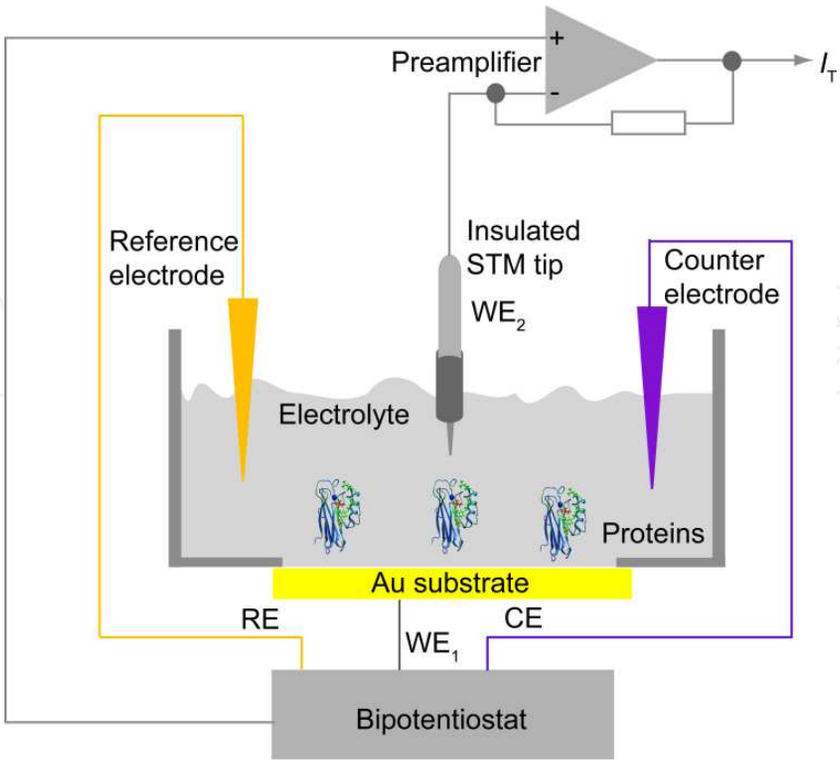

Figure 2. EC-STM configuration, the bipotentiostat controls potential of tip and sample with respect to reference electrode.

brium with the corresponding metal cation in solution. In the past decade, STM has been applied to study the solid-liquid interfaces, in which the STM probe is immersed into the liquid media and controlled by the electrochemical module of STM for *in-situ* monitoring of redox process on the sample electrode. ECSTM has advantages over classical or conventional STM operated either in air or in a vacuum. It allows precise and independent control of both tip potential and sample electrode potential through the use of a bipotentiostat and a quasi-reference electrode [28]. Generally, STM allows to perform electronic spectroscopy by recording the tunneling current (I_t) with the applied bias potential (V_b) known as scanning tunneling spectroscopy (STS) and the same can be applied in electrochemical environment, leading to electrochemical scanning tunneling microscopy (ECSTS) technique [29]. Even though ECSTS is a sophisticated and powerful tool it is not widely used because of complexity in tip preparation methods.

Generally in ECSTS, the current flowing through the tip has several components; a) STM tunneling current, b) faradaic current by the electrochemical reaction at the tip/electrolyte interface and c) charge-discharge process of the electrochemical double layer at the tip-electrolyte interface. So, if the faradaic currents and the charge-discharge processes are larger than the set-point tunneling current, the STM measurement will no longer be possible. Hence there should be an alternative to eliminate these two electrochemical contributions to the measured tip current. The most effective alternative is, taking the advantage of the fact that faradaic/capacitive currents are directly proportional to the exposed area of the electrode,

coating the tip except for the very apex so that tunneling current can flow while faradaic and capacitive currents can be minimized [30,31]. Generally in STM, the tunneling current is usually set to between 1~10 nA. For accurate measurements, coated tips must yield faradaic and capacitive currents ≤ 0.1 nA at the end of the STS curve when ramping at the highest tip potential scan rate (up to 10 V/s) needed to minimize drift, whereas the STS curve is recorded without feedback. Various methods and materials have been proposed for coating purposes, such as apiezon wax, melt glass, copolymers, and a combination of glass and polymer, and in all these coating procedures, the faradaic and capacitative contributions are too large to be subtracted from the measured tip current, and thus, they do not allow STS spectra to be under electrochemical control [32].

As mentioned above, the electrochemical charge associated to the charging-discharging process of an electrode in contact with a specific electrolyte depends directly on the exposed area of the electrode itself. For this purpose, the ECSTM tips must be insulated from the electrolyte, in the way that just the very end tip apex remains in contact with the electrolyte. With this isolation process, the electrochemical current measured through the STM must be better than 10 % of the tunneling set point current, that is, typically ≤ 0.1 nA. Electrophoretic paints are increasingly used for coating Pt-It tips as they are chemically and electrochemically inert insulators [33]. However, among many protection methods available, apiezon wax is still used for ECSTM tip isolation, despite its disadvantages.

4. Characterizations with ECSTM

4.1. Understanding electrochemical processes such as corrosion, deposition, and adsorption

Applications of ECSTM in the field of corrosion have mainly focused on understanding the mechanism of corrosion initiation and the process of inhibition, including pitting initiation, surface dissolution, passive film formation, and the effect of inhibitors. ECSTM has been utilized to study a variety of materials, including Cu, Ni, and Fe, in many different corrosion environments [34]. In general, the term *corrosion* stands for material deterioration or surface damage in a liquid environment. In the case of metals, it is basically a chemical/electrochemical process that suggests an oxidation of a metal which transfer electrons to the electrolytic environment and undergoes a change of valence from zero to a positive value [35]. Normally, this initial process leads to a number of parallel electrochemical methods that result in material dissolution and/or eventual formation of secondary corrosion products. Basically the metal corrosion processes can be classified in two different forms: one is general corrosion [36] that symbolizes those corrosion processes involving the entire surface area of the material, and the second one localized corrosion [37] which mentions to a number of corrosion processes that are triggered at specifics sites on the material surface. The presence of a surface passive film prevents the metallic substrate from further oxidation, i.e., the surface becomes passivated. However, the passive state of a metal under certain conditions is susceptible to localized instabilities that prompt the corrosion of the metal electrode through the local dissolution of the passive layer. This process is called as pitting corrosion [38].

http://dx.doi.org/10.5772/57236

Pitting corrosion takes place at passivated metal surfaces and leads to a creation and growth of an active *pit* [39]. It is quite common that these pits can easily develop at defective sites on the passive film surface, on sharp edges or sites where the oxide film is thinner. The essence of the pitting process relays in its anodic nature (metal dissolution) compared with a passivated cathodic region surrounding it, thus allowing the continuous flow of electrons to take place [40]. The pit formation is depicted in Fig. 3 where peaks indicate the pitting corrosion. Most metal passive layers present a semiconducting or insulating electronic behavior and, therefore, it is expected to understand the initiation of the pitting corrosion process, this requires to embed semiconductor phenomena into an actual classical corrosion mechanisms.

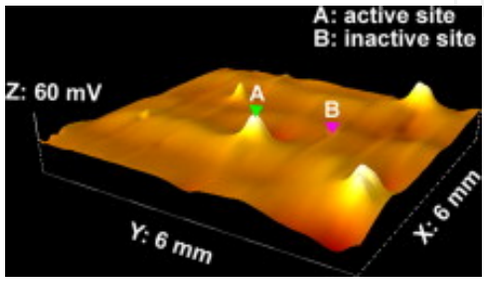

Figure 3. The typical 3D potential distribution image for the stainless steel in 10% (wt.%) $FeCl_3$ solution. Figure reproduced with permission from: ref. 43, © 2012 Elsevier

It is known that, charge injection always occurs at high electric fields in particularly under dc conditions. The presence of space charge in solid dielectrics will result in distortion of electric field distribution. Dielectric breakdown can began in the region where electric field enhancement takes place if the electric field exceeds the "threshold strength" of the material. That is, spontaneous generation of extra charge carriers in an electrically insulated region either by tunneling (Zener breakdown) or by collision (avalanche breakdown) [41]. Both these mechanisms occur when a sufficiently high electric field is applied to the oxide layer thus generating high currents passing through the interface.

The location of a carrier at the semiconductor solid surface is generally accounted as the lattice bond weakening that ultimately lead to the bond breaking and the corresponding electrochemical electrode corrosion (dissolution). This process may continue in different routes that comprise either the movement of electrons and holes to charged states [42]. The rate of these charge carriers (e^- and h^+) arriving to the particular charges state will then govern the dissolution rate and, consequently, the material corrosion. ECSTM can be used to analyze the pitting corrosion by measuring potential distribution image for the stainless steel in 10% (wt.%) $FeCl_3$ solution after 30 min of immersion [43]. Further, ECSTM is able to map the in-situ pitting process with micro and nano-spatial resolution and can locate the positions also the local activity of pitting corrosion in an early stage.

ECSTM has been a valuable tool for understanding electrochemical processes such as corrosion, deposition and adsorption. For example, a method to estimate the pitting corrosion of naked and self-assembled monolayer (SAM) of n-alkane thiol modified Au (111) surfaces in CN^- solutions was examined [44]. It is estimated that SAMs reduced the rate of corrosion, but

fragile and contain too many defects. To estimate this corrosion, the applied potential was slowly changed from negative to positive values and it is observed that at small positive potential values leads the initial stage of corrosion, at slightly higher positive potentials pits and step edges occurs and even higher potentials the etching starts and surface becomes rough [45]. Overall, the SAM modified surface is more resistance to corrosion for longer periods of time and at more positive (etching) potentials than the naked Au surface. Hence, 1) the potential imaging technique is able to locate the positions and map local activity of the pit initiation. Hence ECSTM study becomes an alternative method for analyzing the pitting initiation at an early stage; 2) combined with potential imaging, *in situ* ECSTM can be useful for imaging the surface topographies that associated with dynamic process of local breakdown of passive layers and micropitting initiation; 3) a threshold potential can be defined as a critical potential to characterized the local breakdown of passive layers; 4) the pitting initiation is strongly depends on the surface conditions of passive film, concentration of the ions and pH in the solution.

4.2. Molecular resolution imaging of redox species in solution with ECSTM

In biological molecules, electron transfer (ET) in solid surface or liquid solution can occur between donor (D) and acceptor (A) separated by a long distance. To describe this process quantitatively, sophisticated models are required. Additionally, scanning tunneling and atomic force microscopy (STM and AFM, respectively) have opened an exciting new perspective for molecular imaging. STM imaging at the solid/air interface to molecular and occasionally sub molecular resolution also has been extended to biological macromolecules including DNA and a number of redox and non-redox proteins [46,47]. *In-situ* STM offers, on the other hand, new electrochemical spectroscopic probes in addition to current-bias voltage relations, particularly the relation between the tunnel current and the overvoltage of both the tip and substrate electrodes relative to a common reference electrode. Particularly, *in-situ* scanning tunneling microscopy (STM) of redox molecules, in aqueous solution, shows interesting analogies and differences compared with interfacial electrochemical electron transfer and also in homogeneous solution. With ECSTM, high resolution imaging and spectroscopy of adsorbed molecules can be achieved. It is understood that ECSTM combines electrochemical control and STM high-resolution profiles such as molecular imaging and scanning tunneling spectroscopy (STS) [48]. The possibility of using ECSTM to observe single-molecule charge transport was proposed in the early 1990s. The first ECSTM experiments was performed on iron porphyrin molecules adsorbed on highly ordered pyrolytic graphite (HOPG) surface, and the redox-tuned resonant tunneling effect was directly visualized by STM imaging [49]. Since then, it has become a powerful tool to study the interfacial electron transfer and molecular conductance of electro active species at single-molecule level in an electrochemical environment. For conductance imaging, with *in situ* ECSTM mapping was performed on redox molecules such as azurin (a redox protein) seen in reference [50]. To observe the electron transfer properties and its imaging, Azurin (Az) is a blue single-copper protein adsorbed on gold surface which functions as an electron carrier physiologically associated with oxidative stress responses in bacteria (e.g., *Pseudomonas aeruginosa*) and is a long-standing model for

http://dx.doi.org/10.5772/57236

exploring electron tunneling through protein molecules was studied. The molecular assembly for the effective coupling of Azurin with gold surface can be examined with STM imaging or by examining the electrochemical property of the adsorbed Az on Au surface. Moreover, the combination of electrochemical and STM measurements thus provide a way to quantify one of the fundamental and long-lasting questions in adsorption chemistry of redox proteins: Such as mainly 1) what percentage of the protein molecules retains their biological activity in the immobilized state? 2) In addition to fast ET, stability is another key factor determining reproducibility and operation in applications of the system to molecular electronics. ECSTM enables to observe single-molecule current-voltage relations by tuning the over potential across the equilibrium redox potential. The energy state of both the substrate and the tip in ECSTM is under control by electrochemical potentials relative to a common reference electrode in an aqueous buffer environment [51,52]. This STM configuration is particularly suitable for *in situ* mapping of electronic properties of redox proteins during their biological action (e.g., ET or electrocatalysis), because the aqueous phase is essential for almost all biological processes in nature. STM imaging was performed to observe single molecules, for which high-resolution images of Az was obtained by keeping a constant bias voltage between the substrate and the tip, with the substrate potential set at the equilibrium redox potential (zero over potential) of azurin. Imaging was performed toward either positive or negative overpotentials by adjusting the substrate and tip potentials in parallel (i.e., at constant bias voltage) and finally was returned to the equilibrium potential [53]. The adsorbed azurin monolayer is sufficiently robust and can withstand repeated ECSTM imaging without loss of its activity. Hence, a series of STM images was obtained at various overpotentials. Fig. 4 shows typical images in which three molecules were targeted. Focus is on the central molecule; two molecules in the upper left region serve as a positioning reference. The single-molecule contrast is clearly tuned by the redox state of azurin, with a maximum around the equilibrium redox potential (Fig. 4C). The contrast decreases upon applying either positive (Fig. 4 A,B) or negative (Fig. 4 D, E) overpotentials, but the effects are not symmetric, with the decay being stronger at negative overpotentials.

4.2.1. Conductance images by potential variation

Potential-dependent EC-STM images of azurin was provided by an experiment in which azurin was chemisorbed on Au substrates studied by EC-STM [54]. *In-situ* cyclic voltammetry (CV) measurements were performed on monolayers of azurin to confirm that protein retained its redox activity and to examine the redox potentials. As proposed by Kim et. al., azurin adsorbed on Au surface has the redox peaks at with anodic redox wave at E_{pa}= 278 mV and cathodic wave at E_{pc}= 486 mV which corresponds the redox process of $Cu^{2+/1+}$ center in Azurin [55]. The open circuit potential (E_{oc}) of the cysteine-modified azurin on Au surface was found to be 80 mV. So, these three states were utilized to examine the images of azurin under different potentials. Typical bright spots are seen when tuning the substrate potential in a region, appear to be strongly potential-dependent of redox potentials. Such kind of behavior is consistent with a resonant nature of the current measured in STM experiments in the Au adsorbed azurin molecules.

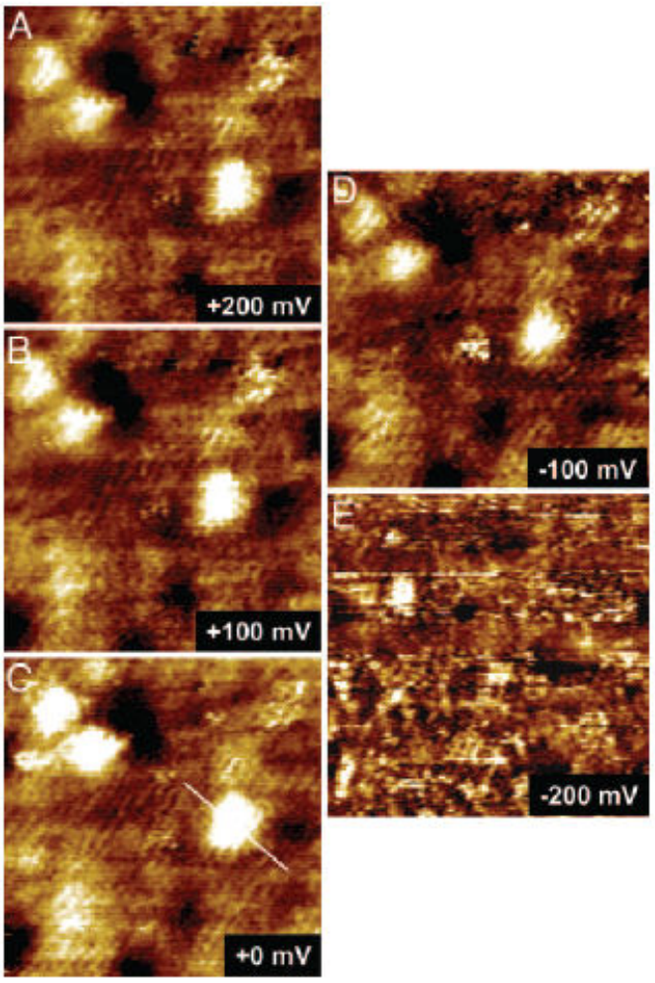

Figure 4. A series of STM images showing the *in-situ* observations of the redox gated electron tunneling resonance arising from the single azurin molecules. The images were obtained by using the azurin/thiol linker/Au at a fixed bias voltage of -0.2 V. by the substrate potential by (a) +200 (b) +100 (c) 0 (d) -100 and (e) -200 mV respectively. Scan area is 35×35 nm. Figure reproduced with permission from: ref. 27, © 2005 The National Academy of Sciences.

The single-molecule tunneling contrast is clearly measured by the redox state of the protein; the experimental observations represented in Fig. 5(a-c) can be explained by a two-step electron transfer mechanism in the STM redox process. The energy levels of the substrate electrode, the tip, and a redox molecule located in the substrate-tip gap may all be modified by changing the substrate potential, but the difference between the substrate and tip energy levels will remain constant if the bias voltage is fixed as the experimental conditions applied [56]. As a consequence, the redox level is shifted relative to the substrate and tip Fermi levels. The tunneling current (I_t) is gated by the molecular redox level, which is displayed directly by the changes in STM contrast. In other words, the contrast changes observed are due to the redox gated tunneling resonance. In contrast, the bias voltage will change with changing the substrate potential when the tip potential is fixed. The molecular energy levels can be mostly located either above or below the tip Femi level, resulting in no significant resonant tunneling tuned by the substrate potential.

http://dx.doi.org/10.5772/57236

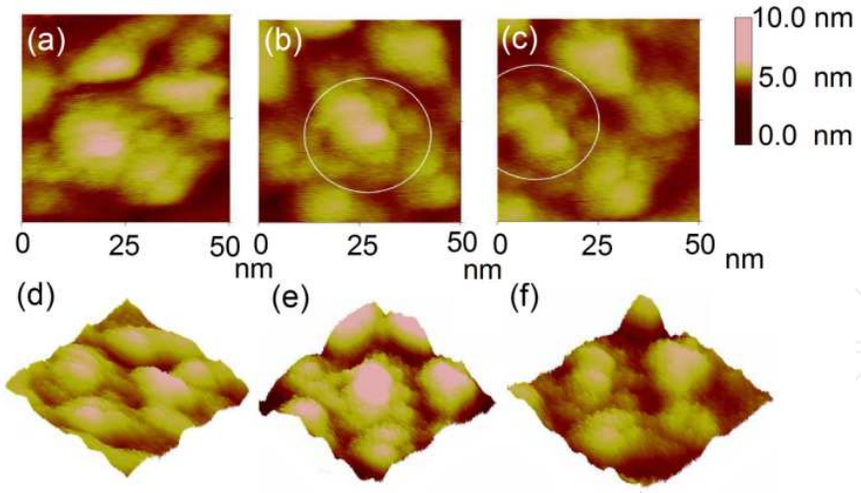

Figure 5. Sequence of ECSTM images obtained for immobilized azurin molecules on Au substrate for different bias potentials; (a) OCP (80 mV) (b) oxidation (486 mV) (c) reduction (278 mV) respectively. Scan size is 50 nm (d-f) is the 3-dimentional profile of (a-c) images respectively. Figure reproduced with permission from: ref. 30, © 2010 Elsevier

The tunneling current (I_t) dependence on the effective overpotential ($e\xi\eta$) and the bias voltage (eV_{bias}) can be analysed in steady-state electron transfer form in the following combination [50]

$$I_t = 2en\frac{k^{o/r}k^{r/o}}{k^{o/r}+k^{r/o}} \tag{2}$$

where $k^{o/r}$ and $k^{r/o}$ are the rate constants, for electron transfer between the tip and protein and between the protein and substrate respectively. n is the number of electrons transmitted in a single electron transfer event and e the electronic charge.

$$k^{o/r} = \kappa_t\rho_t\frac{\omega_{eff}2k_BT}{\alpha_t}\exp\left(-\frac{\left(\lambda - e\xi\eta - e\gamma V_{bias}\right)^2}{4\lambda k_BT}\right) \tag{3}$$

$$k^{r/o} = \kappa_s\rho_s\frac{\omega_{eff}2k_BT}{\alpha_s}\exp\left(-\frac{\left(\lambda - eV_{bias} + e\xi\eta + e\gamma V_{bias}\right)^2}{4\lambda k_BT}\right) \tag{4}$$

where κ_t and κ_s are electronic transmission coefficients for electron transfer between the tip and the protein, and between the protein and the substrate, respectively; ρ_t and ρ_s are the electronic level densities of the tip and the substrate; ω_{eff} is the effective nuclear vibrational frequency, α_t and α_s are the transfer coefficients for electron transfer between the tip and the protein and between the protein and the substrate, respectively; λ is the reorganization free

energy; ξ is the fraction of the substrate-solution potential drop, η is the overpotential; γ is the fraction of the bias voltage drop at the site of the molecular redox center. It should be noted that, the parameters ξ and γ represent the electric potential distribution in the ECSTM tunneling gap.

4.2.2. Current-voltage characteristics and transition voltage spectroscopy of individual redox proteins

The measurement of I-V plots is essential for electrical characterization of devices, particularly in redox proteins by electrochemical scanning tunneling microscopy (ECSTM) is essential for the development of bioelectronic devices and biosensors. Further transition voltage spectroscopy (TVS), through which molecular level positions can be examined in molecular devices without applying higher voltages, was utilized for organic monolayer and also for non-redox proteins. For the first time, see [57] TVS spectroscopy for redox proteins which is useful for understanding voltage dependence of molecular conductance is specifically important for the mechanism of ET in redox-active molecule.

ECSTM was employed to measure the I-V characteristics of the redox protein azurin covalently bound to Au substrate in an electrochemical cell under bipotentiostatic control for the probe and sample electrodes versus Ag/AgCl reference electrode on both the reduced and oxidized azurin molecules. I-V measurements were carried out in the tunneling configuration (better known that there is no physical contact between the STM probe and the protein) and the wired configuration (where the probe is in contact with the protein). In tunneling configuration of ECSTM, like normal STS spectroscopy, the I-V curves were obtained by positioning the probe over a region with a high protein surface concentration once the imaging is finished. The I-V curves for the reduced azurin depicts two distinct behavior one relatively linear and the other more rectifying behavior which is not observed on bare Au electrode.

This rectifying behavior is due to the applied bias voltage such as the reduced and oxidized states of azurin. From the I–V characteristics, the conductance (G) of the tunneling gap in the presence of azurin was calculated from the relation G = I/V to be between 10^{-6} G_0 and 10^{-5} G_0. To get better understanding of the obtained I-V curves, TV value that can be used to describe the electrochemical potential dependence of the azurin conductance in the framework of TVS. Individual I-V curves and plotted $\ln(I/V^2)$ versus 1/V displayed a minima in the curve, called transition voltage(TV) value, Fig. 6, which is not visible in bare Au samples. Several ET studies of redox molecules have shown that a transition in conductance occurs when the application of an external potential results in the arrangement of the molecular energy levels and the Fermi level of the electrodes. Here, the low TV value found for azurin suggests that the effective barrier for tunneling through a solution is lower than the barrier observed in pure tunneling processes is in agreement with experimental and theoretical works on tunneling through an electrochemical environment [58,59].

In particular, in the context of two-step ET in a redox molecule, a transition was predicted by theory to occur in the range where the effective voltage in the redox center is higher than the reorganization energy of the molecule.

http://dx.doi.org/10.5772/57236

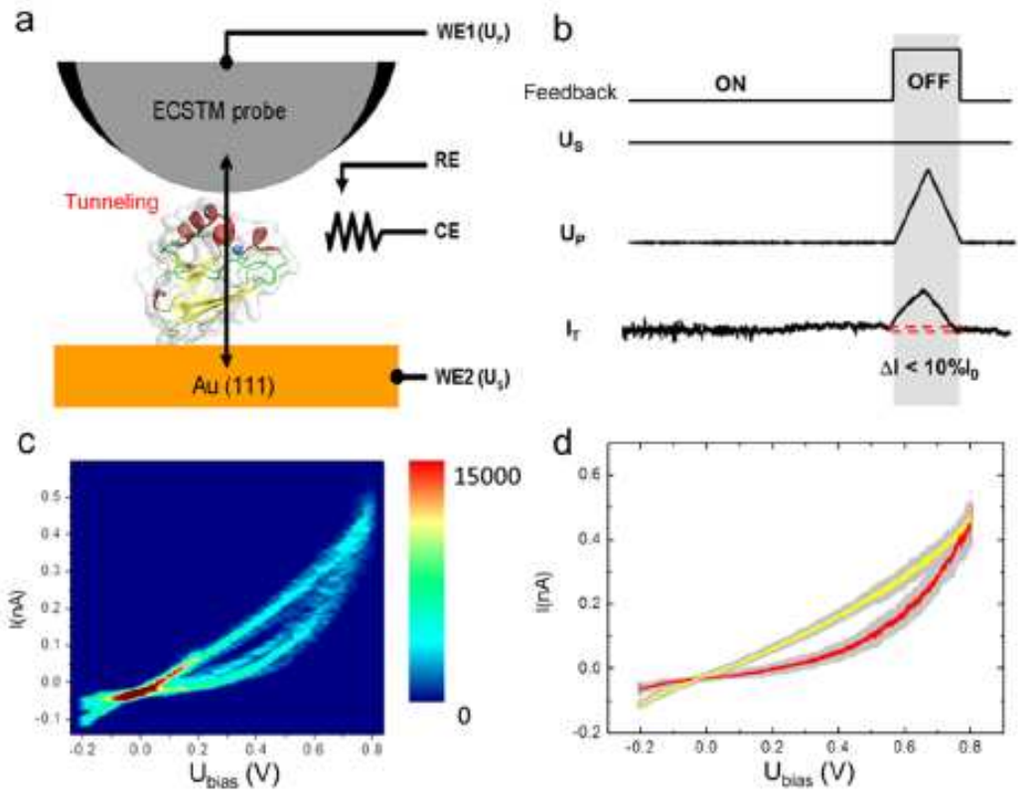

Figure 6. (a) Experimental ECSTM set-up for the azurin immobilized Au structure, WE, working electrode, RE, reference electrode, CE, counter electrode. (b) I-V curves, a triangular ramp was applied to the probe (WE_1) while the feedback is off. The current signal (I_T) was recorded at constant potential (WE_2). (c) 2D I-V histogram showing two populations of curves in azurin on Au. (d) Average of two I-V curves obtained in (c) corresponding the azurin (red curve) and bare Au (yellow curve). Gray error bars indicate the standard deviations. Figure reproduced with permission from: ref. 31, © 2012 ACS

For the determination of TV in the conductance of the redox protein, the tunneling current for the two-step electron transfer mechanism, I_T is given by [60],

$$I_T = e\kappa\rho(eU_{bias})\frac{\omega}{2\pi}\left\{\exp\left[\frac{e}{4\lambda kT}\left(\lambda+\xi\eta+\gamma U_{bias}\right)^2\right]+\exp\left[\frac{e}{4\lambda kT}\left(\lambda+U_{bias}-\xi\eta-\gamma U_{bias}\right)^2\right]\right\}^{-1} \quad (5)$$

in which κ is the electronic transmission coefficient; ρ is the density of states in the metal near the Fermi level; ω is the nuclear vibration frequency; k is Boltzmann's constant; T is the temperature; $U_{bias} = U_P - U_S$ is the potential difference between probe and sample electrodes; λ is the reorganization energy; η is the overpotential, given by $\eta = U_S - U_{Az}$, where U_{Az} is the redox potential of an azurin molecule; and γ and ξ are two model parameters describing the shifts in U_{bias} and η at the redox center, respectively. The parameters γ and ξ are related to the electronic coupling of the molecule with the probe and substrate, respectively

To obtain values of the parameters for azurin, the experimental I-V curves has been fitted using Pobelov and Wandlowski's numerical equation,[61]

$$I_T = 1820\kappa U_{bias}\left\{\exp\left[\frac{9.73}{\lambda}\left(\lambda+\xi\eta+\gamma U_{bias}\right)^2\right]+\exp\left[\frac{9.73}{\lambda}\left(\lambda+U_{bias}-\xi\eta-\gamma U_{bias}\right)^2\right]\right\}^{-1} \quad (6)$$

in which I_T is expressed in nA, potentials are in V, and λ is in eV. In this expression, typical values for ω in a liquid and ρ in a metal were used, and ξ, γ, λ, and γ were left as free model parameters. In the wired junctions, a TVS spectrum is also determined but a negative low value was determined. This minimum is due to the stronger coupling with the probe electrode, which lowers the energy barrier between the levels of the STM probe electrode and the molecule. Thus, in wired junctions, the TV is related to the contact resistance, as commonly found for single-molecule junctions. Hence, these measurements help in characterizing redox proteins and understanding their performance in biological ET chains and molecular electronic devices.

5. Applications of ECSTM

5.1. Combined instrument for electrochemical scanning tunneling microscopy (ECSTM) and scanning electrochemical microscopy (SECM)

Until now, we have analyzed the advantages of ECSTM but there are many versatile techniques such as scanning electrochemical microscopy (SECM) which is also a useful tool to analyze interfacial physicochemical processes. The main reason, ECSTM is able to localize electrochemical reactivity only if this is accompanied by changes in sample topography, e.g. for deposition, adsorption or dissolution reactions. Parallel to the advance of ECSTM, scanning electrochemical microscopy (SECM) was developed as a new tool for localized electrochemistry [62,63]. SECM uses an ultramicroelectrode (UME) as a probe and by either amperometric/potentiometrically utilized to investigate the activity and/or topography of an interface on a localized scale. The tip moves much longer distance than the tunneling distance and measures faradic currents that results from an electron transfer reaction at UME [64,65]. Several operational modes of SECM have been developed which allows the investigation of local chemical properties of interfaces. To study biomolecular interfaces these are most important methods which can be utilized for the analysis.

a. *Tip detection (or collection) method:* Local variations in concentrations about an interface can be mapped with both potentiometric and amperometric probes. In this method, the detector probe is generally assumed to be passive (i.e. non-perturbing to the interfacial process) [66]. Tip detection measurements have demonstrated particularly powerful in identifying localized transport pathways in synthetic membranes and biological tissues. Also it is useful for the investigation of the activity of immobilized enzymes [67]. However, mass transport between the tip and the surface, under tip detection conditions, is complicated.

b. *Feedback mode:* SECM involves in the usage of the tip to locally perturb an interfacial process, by electrolysis or ion transfer, and determine the kinetic effect from the resulting

http://dx.doi.org/10.5772/57236

tip current. A mediator is added (concentration in mM) to the supporting electrolyte that is converted at the UME under diffusion controlled conditions which produces a steady-state current, I_T,∞, in the bulk phase of the solution. If the UME is brought close to an inert and insulating surface, it blocks the diffusion of the mediator to the UME and the UME current I_T decreases below I_T,∞ (called negative feedback) [68]. If the UME is brought above a conductive surface or a catalytically active surface, I_T increases above the value found for an inert and insulating surface. The magnitude of this increase depends on the local reactivity of the sample. A diffusion-controlled reaction at the sample and the tip constitute an important limiting and is called as positive feedback [69].

c. *Advanced tip positioning:* SECM tip usually needs to be positioned close to an interface with high precision. Accurate positioning is achieved by attaching the tip to piezoelectric translators. However, this still leaves the problem of determining the exact separation of the tip electrode and the surface commonly known as '*distance of closest approach*' of the electrode with the surface [70]. One can use the amperometric response of the tip electrode in some instances for many systems it might be difficult to add a redox-active species to the solution, without affecting the process or the viability of the sample. Also there are challenges that include in low analytes concentrations or background processes in biological media which means it is hard to measure the distance accurately from the amperometric response [71]. Hence, much effort has been directed towards the development of alternate procedures for tip positioning and distance determination.

Shear force modulation is one method to achieve the control of tip-sample separation by shaking the electrode through a small oscillation in the *x-y* plane. As the electrode is brought close to a surface, the oscillation is damped, to a degree which depends on the tip-substrate separation. Images are usually acquired at constant damping amplitude, which resembles to a constant distance between the tip and substrate; thus, the tip follows the surface contours [72]. Further, Tip position modulation SECM refers to an operation where an amperometric tip is oscillated in a sinusoidal motion perpendicular to the surface. The resulting current varies with the frequency of the driving oscillation. The amplitude and phase of the oscillating current enable one to deconvolute the activity and topography of the surface [73]. The phase of the current is the same as the phase of the tip-surface separation when the probe is oscillated above an inert surface, whereas they are entirely out of phase above a conducting surface (in positive feedback mode).

d. *SECM with ECSTM*: SECM coupled ECSTM has the dual benefits of nanometer scale resolution imaging along with the ability of the electrochemical measurements. For example see [74]. In order to perform measurements with SECM at nanometer scale many number of technical hurdles has to overcome. Some of them are 1) preparation of suitable nanoscale electrodes with insulator coatings 2) scanning and positioning the probe above the sample surface with a sample distance of 10 nm which is much larger than the tunneling distance but smaller than some electrode radii of the probe, while avoiding mechanical contact between sample and probe. In order to observe electrochemical reactivity at individual nanometer-sized features, such features have to be prepared on the sample surface with such a large distance that SECM can determine the signals of

individual features. But it is very difficult to avoid the possibility of mechanical contact between the probe and the surface structures. Hence a method is adopted in which the probe is used in ECSTM mode over the protruding regions of the sample surface and retracted from there [75]. A novel instrumentation has been developed for the imaging with ECSTM and SECM with Pt/Ir wire coated with paint is used as the tip. The tip is kept at a working distance of 20 nm which is much larger than the tunneling distance but enough for feedback imaging for SECM. Probes for the operation of ECSTM and SECM is the most important factor so selecting a desired probe is crucial for better imaging and electrochemical analysis. Tips can be distinguished by the geometric shape of the active electrode area and the insulating sheath for different applications.

Disk-shaped microelectrodes which are the preferred shape for quantitative SECM experiments in the micrometer range, which consists of a Pt wire, sealed in glass or quartz with a laser-heated capillary puller (Fig. 7a) [76]. Because of the large insulating sheath these electrodes are unlikely to function as ECSTM probes. Ring-disk electrodes have been approximated as modified cantilevers for combined scanning force microscopy (SFM)/SECM experiments (Fig. 7b) [77]. The probes have been produced by modification of SFM cantilevers and shaping individual cantilevers by fast ion bombardment. The outer electrode was square-shaped with a side length of 1.5 mm.

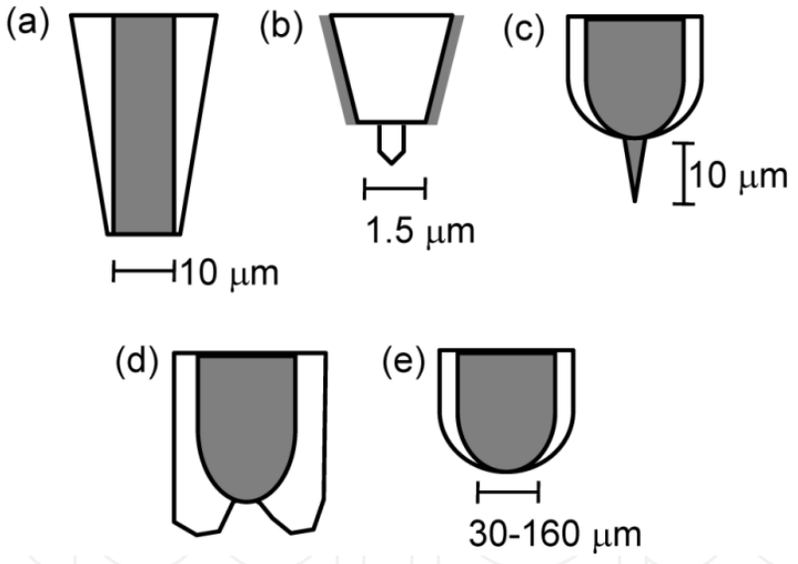

Figure 7. Schematics of the shapes of different microelectrodes used in scanning probe microscopy. Figure reproduced with permission from: ref. 40, © 2010 Elsevier

Electrodes shown in Fig. 7c are generally used for high-resolution ECSTM experiments. The pointed tip allows atomic resolution in tunneling experiments. However, the active electrode area is decreased by an insulating coating which leaves the pointed area of about 10 mm length open. This is sufficient because the potentials for the imaging experiments are selected such that no Faradic reactions proceed at the tip potential. The tunneling current can be as high as 1 nA so that other currents do not interfere significantly with the experiments. Such electrodes are, however, not useful for SECM feedback experiments. Mediators can access the UME by

http://dx.doi.org/10.5772/57236

diffusing parallel to the sample so that no diffusional blocking occurs above passivated samples [78]. The positive feedback would be insignificant compared with the large background current from mediator conversion at such electrodes. Electrodes with a slightly recessed active electrode area (Fig. 7d) were used for amperometric single molecule detection. No images were recorded with such probes. For the combined ECSTM/SECM operation the electrodes such as in Fig. 7e are required. Although they are not as pointed as the one in Fig. 7c, they should allow ECSTM experiments of flat samples although not with atomic resolution. Apart from that, the shallow cone would still provide a blocking of the mediator diffusion above passivated samples [79,80].

Operating principle:

The combined ECSTM/SECM operation is based on the sequential acquisition of ECSTM and SECM [74] data shown in Fig. 8. Once the probe is brought in tunneling contact, an ECSTM image is recorded in the constant current mode. It provides topographic data of the sample. After completion of the ECSTM scan, the electronic feedback loop is switched off and the probe is retracted 20 nm from the working point of the ECSTM scan. This distance is much larger than the tunneling distance. At the same time the potentials at the probe are switched for a desired range to obtain the redox properties of the adsorbed molecule on the surface. After completing the SECM scan, the probe is brought back into tunneling contact with the sample and a step perpendicular to the high-frequency scan axis is performed. From there the sequence is repeated until a full image frame is recorded.

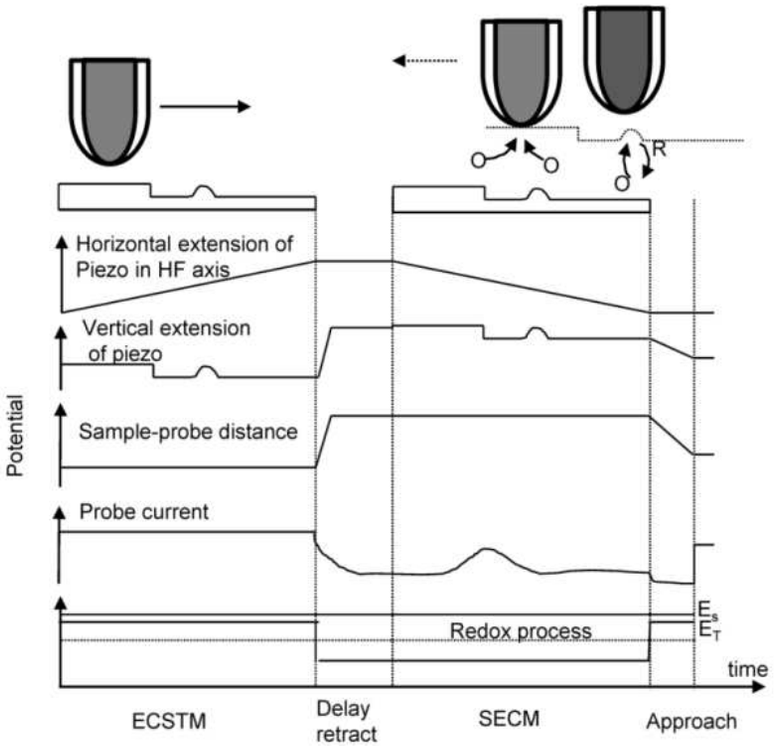

Figure 8. Schematic diagram for the combined operation of ECSTM-SECM performance. Figure reproduced with permission from: ref. 40, © 2010 Elsevier

5.2. Limitations of ECSTM

ECSTM has several limitations and drawbacks, generally these limitations resides in the difficulty to perform bias-dependent measurements such as when potential of the substrate is fixed during electrochemical process then the tip is adjusted to maximize the faradic current and to optimize STM measurements, with the tunnel voltage is no longer adjusted over long range. Hence in STS measurements, voltage dependent imaging is not possible to measure in ECSTM mode [81]. Limitations are also arises from the possible interference of the tip with the electrochemical process at the working electrode. The close proximity of the tip causes shielding effects for reaction at the sample-solution interface.

Further, corrosion studies by ECSTM are also facing problems as high rate of mass transport with respect to time for acquisition of images thus leads to low resolution images. Apart from these limitations, ECSTM is an effective tool which can provide valuable information related to molecular structures of the adsorbed molecules at nanoscale and also provide information relating to corrosion process like adsorption, dissolution and localized corrosion of metallic materials.

5.2.1. Instability and drift

Repeated electrochemical experiments on the all the coated tips leads two typical instability behaviors. A progressive increase of the maximum current is observed on aging, which is associated with dissolution of the coated layer that leaves more and more metal surface uncoated in time. Secondly, all the current levels at each potential drift in time toward higher values, which means that the effective electrical resistance at the tip due to coating decreases. Probably, the solution was leaking into the interface between metal and coating [82].

Mechanical drift is a critical parameter in high resolution imaging caused by the differential thermal expansion of individual instrument components. Sources of drift in the X-Y plane consist of these thermal effects and hysteresis in the piezo-scanner. The Z-direction presents a more complex situation due to the contributions of temperature, sample tilt in the X-Y plane, and hysteresis. Further, in the cases of *in-situ* and electrochemical experiments where drift is typically higher [83], the effects of time and evaporation of the solvent must be carefully balanced. The influence of drift in the X-Y plane detrimentally affects two main aspects of the imaging process. First, the ability to image a given region or feature over time is limited. Second, high-resolution imaging of atomic and molecular lattices demonstrates curvature in the observed periodic structure. The analysis of drift in the X-Y plane is carried out by the collection of sequential images [84].

The major effects of drift in the Z-direction are most disruptive during surface spectroscopic measurements. In the STM application, tunnel current versus distance curves (I-S) collected at a constant bias voltage provide a direct measurement of the effective local barrier height involved in the tunneling process. This value is generally unknown and directly influences the more common bias-dependent (I-V) spectroscopy. It is therefore desirable to minimize differential drift in the Z-direction between the tip and sample. Measurement of drift in the Z-direction was quantified through long-term acquisition of the Z-signal in the tunneling condition.

5.2.2. Poorly resolved images

High-resolution imaging has been the primary feature that attracted the researcher's attention to scanning probe microscopy yet there are still a number of outstanding questions regarding this function of scanning tunneling microscopes or coupled with other microscopic techniques. Some types of proteins may adhere to the tip. This will reduce resolution giving "fuzzy" images. If tip contamination is suspected to be a problem, it will be necessary to protect the tip against such contamination [85]. The ECSTM images become unclear and noisy at potentials more negative potentials due to the perturbation of the tip caused by severe reactions. A great quantity of spots will be observed on all over the surface. In addition, it is know that on the surface of graphite substrate the alkane molecules are assembled in flat-lying lamellar structures. The alkane adsorbates on graphite were analyzed by means of a droplet of saturated alkane solution that is deposited on graphite surface and the metallic tip penetrates this droplet and a molecular adsorbate at the liquid-solid interface until it detects a tunneling current. At these conditions the tip is scanning over the ordered molecular layer in immediate vicinity of the substrate. A specific feature of the STM imaging at the liquid-solid interface is that the probe is surrounded by the alkane saturated solution [86]. Any instability of the imaging and the use of low tunneling gap resistance cause a mechanical damage of the alkane order, and the probe might record the image of the underlying graphite. If the gap is increased again the alkane order is restored. It is difficult to get STM images of "dry" alkane layers on graphite because an occasional damage of the layer is not repairable. This progress relies on instrumental improvements (better signal-to-noise characteristics, low thermal drift, improved detection and control of the tip-sample forces, etc.) and the use of sharp probes [87].

The other issue is related to the better understanding of the nature of atomic-scale resolution in STM. In some cases, imaging provides only the lattice resolution in the contrast with true atomic resolution where a detection of such defects is expected. The imaging of the periodical lattices with the defects can be demonstrated with the results of the computer simulation which revealed that visualization of the defects does not necessarily mean that the surrounding molecular order is correctly reproduced in the images. These findings emphasize a need of a thorough interaction between the experiment and theory in the analysis of the atomic scale data.

6. Future trends and applications

The invention of the scanning tunneling microscope had a revolutionary influence on the development of material characterization at nanometer scale. The future of STM with electrochemical control depends on the development of appropriate probes for implementing the electrochemically controlled current sensing atomic force microscopy (ECAFM) [88]. In comparison of ECAFM and ECSTM, it can be said that both methods can measure the electronic properties of single molecules but ECAFM allows the control of force applied by the tip on the molecules adsorbed on the surface, thus allowing measure the mechanical properties of the single molecules. In comparison with STM, Atomic force microscopy (AFM) doesn't require conductive samples and tips. AFM has the advantages of measuring the local forces between the tip and the sample surface, including van der Waals, Born repulsion, electrostatic and magnetic forces, friction and adhesion [89]. In electrochemical applications, ECAFM is often

preferred because it is easier to set-up and the obtained topographic information is independent of the conductivity of corrosion materials. Moreover, ECAFM is most often used at submicron level, i.e., at a lower level of spatial resolution that does not require preparation of atomically smooth surfaces as for ECSTM studies. Further, ECAFM can also be combined with a variety of other techniques to analyze corrosion and optimize corrosion protection properties [90]. However in comparison with ECSTM, even though ECAFM doesn't require atomically smooth surfaces like ECSTM and also in ECAFM the cantilever-tip assembly doesn't constitute a fourth electrode through which the electrochemical current that would flow, but there is a disadvantage that in the resonant contact mode, the fluid medium tends to damp the normal resonance frequency of the cantilever which is complicated. Further, the noncontact mode is impractical because the van der waals forces are even smaller making it as a big drawback for biological applications. Such instrument would enable better molecular investigation of electron transfer properties thereby maintaining the molecular conformation. To achieve this spectroscopy, specially designed probes such as insulated conductive probes along with bipotentiostat setup essential. The capability of recording atomic scale features with STM has increased the scope of research to develop other types of STM which provide information about the topography and mechanical, magnetic, electrical properties of the surfaces [91]. The development of these new applications is the design of specific probes, having improved spatial resolution, sensing the desired sample properties and operating in different environments. Developing a highly flexible, compact microscopic system can be easily interfaced with commercial control electronics and integrated with inverted optical microscopy. Simple design architecture enables simple exchange of the probe tip, sample, and scanner while enhancing system resonances and resistance to thermal drift. In recent years, the demand of the applications of ECSTM has greatly increased in numerous fields [92]. ECSTM in combination with SECM has the ability to perform local reactivity imaging simultaneously with ECSTM imaging as well as to induce local electrochemical surface modification in the same setup opens up new perspectives for the investigation of heterogeneous reactions in electrocatalysis at metal clusters and in corrosion processes in a new size regime. Hence with the help of STM, complemented by other characterization techniques, it is reasonable to believe that new advance in building specific and functional surfaces can be achieved in the future.

Author details

Ajay Kumar Yagati[1], Junhong Min[3] and Jeong-Woo Choi[1,2*]

*Address all correspondence to: jwchoi@sogang.ac.kr

1 Research Center for Integrated Biotechnology, Sogang University, Seoul, Republic of Korea

2 Department of Chemical and Biomolecular Engineering, Sogang University, Seoul, Republic of Korea

3 School of Integrative Engineering, Chung-Ang University, Seoul, Republic of Korea

http://dx.doi.org/10.5772/57236

References

[1] Eigler D.M, Schweizer E.K., Positioning single atoms with a scanning tunnelling microscope. Nature 1990; 344, 524-526.

[2] Stroscio J.A, Eigler D.M., Atomic and Molecular Manipulation with the Scanning Tunneling Microscope. Science 1991; 254, 1319-1326.

[3] Binnig G, Rohrer H. Scanning tunneling microscopy. Surface science 1983; 126(1-3) 236-127.

[4] Stolyarova E, Rim K.T, Ryu S, Maultzsch J, Kim P, Brus L.E, Heinz T.F, Hybertsen M.S, Flynn G.W, High-resolution scanning tunneling microscopy imaging of mesoscopic graphene sheets on an insulating surface. PNAS 2007; 104, 9209-9212.

[5] Heim, M, Eschrich, R, Hillebrand, A, Knapp, H.F, Guckenberger, R, Cevc, G. Scanning tunneling microscopy based on the conductivity of surface adsorbed water. Charge transfer between tip and sample via electrochemistry in a water meniscus or via tunneling? Journal of Vacuum Science & Technology B: Microelectronics and Nanometer Structures, 1996; 14, 1498-1502.

[6] Cui, X. D, Primak A, Zarate X, Tomfohr J, Sankey O.F, Moore A.L, Gust D, Harris G, Lindsay S.M, Reproducible Measurement of Single-Molecule Conductivity. Science 2001; 294, 571-574.

[7] Hallmark, V.M, Chiang s, Rabolt, J.F, Swalen, J.D, Wilson R.J. Observation of Atomic Corrugation on Au(111) by Scanning Tunneling Microscopy. Phys. Rev. Lett. 1987; 59, 2879-2882

[8] Bonnell D.A. Scanning tunneling microscopy. Encyclopedia of Materials: Science and Technology 2001, 8269-8281.

[9] Garcia R, Yuqiu J, Schabtach E, Bustamante C. Deposition and imaging of metal-coated biomolecules with the STM. Ultramicroscopy 1992; 42-44, 1250-1254.

[10] Itaya K. In situ scanning tunneling microscopy in electrolyte solutions. Progress in Surface Science 1998; 58, 121-247.

[11] Wang E. Electrochemical scanning tunneling microscopy. Analytical sciences 1994, 10 (1) 155-156.

[12] Binnig G, Rohrer H, Gerber Ch, Weibel E. (111) facets as the origin of reconstructed Au(110) surfaces. Surface Science letters 131 (1) L379–L384.

[13] Sobczyk S, Donarini A, Grifoni M. Theory of STM junctions for π-conjugated molecules on thin insulating films Phys. Rev. B 85, 2012; 205408 (17pp)

[14] Van de leemput, L E C, van Kempen H. Scanning tunnelling microscopy, Rep. Prog. Phys.1992; 55, 1165-1240.

[15] Frommer, J. Scanning tunneling microscopy and atomic force microscopy in organic chemistry. Angew. Chem.1992; 31(10) 1298-1328.

[16] Gross L, Mohn F, Moll N, meye G, Ebel R, Abdel-Mageed W.M, Jaspers M. Organic structure determination using atomic-resolution scanning probe microscopy. Nature Chemistry 2010, 2, 821-825.

[17] Kim Y.-T., Bard, A. J. Imaging and etching of self-assembled n-octadecanethiol layers on gold with the scanning tunneling microscope, Langmuir 1992; 8, 1096-1102.

[18] Halbritter J, Repphun G, Vinzelberg S, Staikov G, Lorenz W. J. Tunneling mechanisms in electrochemical STM -distance and voltage tunneling spectroscopy. Electrochimica Acta, 1995; 40, 1385-1394.

[19] Esplandiu M.J, Carot M.L, Cometto F.P, Macagno V.A, Patrito E.M. Electrochemical STM investigation of 1,8-octanedithiol monolayers on Au(1 1 1).: Experimental and theoretical study. Surface science 2006; 600(1) 155-172.

[20] Gitting D. I, Bethell D, Schiffrin D. J, Nichols R. J. A nanometre-scale electronic switch consisting of a metal cluster and redox-addressable groups. Nature 2000; 408 67-69.

[21] Dieluweit S, Giesen M. Determination of step and kink energies on Au(100) electrodes in sulfuric acid solutions by island studies with electrochemical STM. J. Electroanal. Chem. 2002; 524-525, 194-200.

[22] Funtikov, A.M, Linke U, Stimming U, Vogel R. An in-situ STM study of anion adsorption on Pt(111) from sulfuric acid solutions. Surface Science 1995; 324, L343-L348.

[23] Kunze, J, Strehblow H.-H, Staikov G. In situ STM study of the initial stages of electrochemical oxide formation at the Ag(1 1 1)/0.1 M NaOH(aq) interface. Electrochem. Commun. 2004; 6, 132-137.

[24] Eckhard K, Chen X, Turcu F, Schuhmann W. Redox competition mode of scanning electrochemical microscopy (RC-SECM) for visualisation of local catalytic activity. Phys. Chem. Chem. Phys., 2006; 8, 5359-5365.

[25] Zhang J, Christensen H.E.M, Ooi B.L, Ulstrup J. In situ STM imaging and direct electrochemistry of Pyrococcus furiosus ferredoxin assembled on thiolate-modified Au(111) surfaces. Langmuir 2004; 20(23) 10200-10207.

[26] Pan J, Jing T.W, Lindsay S.M. Tunneling Barriers in Electrochemical Scanning Tunneling Microscopy. J. Phys. Chem., 1994; 98, 4205-4208.

[27] Pobelov I. V, Li Z, Wandlowski T. Electrolyte gating in redox-active tunneling junctions-An electrochemical STM approach. J. Am. Chem. Soc., 2008; 130(47) 16045–16054.

[28] Albrecht T, Moth-poulsen K, Christensen J.B, Hjelm J, Bjornholm T, Ulstrup J. Scanning tunneling spectroscopy in an Ionic Liquid. J. Am. Chem. Soc., 2006; 128 (20), 6574-6575.

[29] Alessandrini A, Facci P. Electrochemical Scanning Tunneling Microscopy and Spectroscopy for Single-Molecule Investigation, Cellular and Subcellular Nanotechnology 2013; 261-273

[30] Zhu L, Claude-Montigny B, gattrell M. Insulating method using cataphoretic paint for tungsten tips for electrochemical scanning tunnelling microscopy (ECSTM). Applied Surface Science 2005; 252, 1833-1845.

[31] Zhang B, Wang E. Fabrication of STM tips with controlled geometry by electrochemical etching and ECSTM tips coated with paraffin. Electrochimica Acta 1994; 39, 103-106.

[32] Guell A. G. Biez-perz I, Gorostiza P, Sanz F. Preparation of reliable probes for electrochemical tunneling spectroscopy. Anal. Chem., 2004; 76 (17), 5218-5222.

[33] Hudson J. E., Abruna h. D. STM and ECSTM Study of the Formation and Structure of Self-Assembling Osmium Complexes on Pt(111). J. Phys. Chem., 1996, 100 (3), 1036-1042.

[34] Díez-Péreza, I, Sanza, F, Gorostizab, P. In situ studies of metal passive films. Curr. Opin. Solid State Mater. Sci. 2006; 10, 144-152.

[35] Ghali E, Dietzel W, Kainer K.-U. General and localized corrosion of magnesium alloys: A critical review. Journal of Materials Engineering and Performance 2004; 13(1) 7-23.

[36] Maurice V, Klein L. H. Marcus P. Atomic Structure of Metastable Pits Formed on Nickel. Electrochem. Solid-State Lett. 2001; 4, B1-B3.

[37] Bolzoni F, Contreras G, Fumagalli G, Lazzari L, Re G. Localized Corrosion: An Empirical Approach to the Study of Passive Film Breakdown Rates. Corrosion2013; 69, 352-363.

[38] Burstein, G. T, Liu, C, Souto, R. M, Vines, S. P. Origins of pitting corrosion. Corrosion Engineering, Science and Technology, 2004; 39(1) 25-30.

[39] Szklarska-Smialowska, Z. Pitting corrosion of aluminum. Corrosion science 1999; 41, 1743-1767.

[40] Kabasakaloğlu K, Kiyak T, Sendil O, Asan A. Electrochemical behavior of brass in 0.1 M NaCl. Appl. Surf. Sci. 2002; 193(1-4) 167-174.

[41] Szklarska-Smialowska Z. Mechanism of pit nucleation by electrical breakdown of the passive film. Corrosion Science 2002; 44(5) 1143-1149.

[42] Rangel C.M, Silva T.M, da Cunha Belo M. Semiconductor electrochemistry approach to passivity and stress corrosion cracking susceptibility of stainless steels. Electrochimica Acta 2005; 50(25-26) 5076-5082.

[43] Ye, C-Q., Hu, R.-G, Li, Y., Lin, C.-J., Probing the vertical profiles of potential in a thin layer of solution closed to electrode surface during localized corrosion of stainless steel. Corrosion Science 2012; 61, 242-245.

[44] Zamborni F. P, crooks R. M. Corrosion passivation of gold by n-alkanethiol self-assembled monolayers: Effect of chain length and end group. Langmuir, 1998; 14(12), 3279-3286.

[45] Marcus P. Surface science approach of corrosion phenomena. Electrochim. Acta 1998; 43, 109-118.

[46] Yagati A.K, Jung M,Kim S.-U, Min J, Choi J.-W. Nanoscaled redox active protein adsorption on Au-dot arrays: An electrochemical scanning probe microscopic investigation for application in nano-biodevices. Thin Solid films 2009; 518(2) 634-637.

[47] Tang L, Li X, Cammarata R.C, Friesen C, Sieradzki K. Electrochemical stability of elemental metal nanoparticles. J. Am. Chem. Soc., 2010, 132 (33), 11722–11726.

[48] Sripirom J, Kuhn S, jung U, Magnussen O, Schulte A. Pointed carbon fiber ultramicroelectrodes: A new probe option for electrochemical scanning tunneling microscopy. Anal. Chem., 2013, 85 (2), 837-842

[49] Tao N.J, Cardenas G, Cunha F, Shi Z. In Situ STM and AFM study of protoporphyrin and Iron (III) and Zinc (II) protoporphyrins adsorbed on graphite in aqueous solutions. Langmuir, 1995, 11(11), 4445-4448.

[50] Chi Q, Farver O, Ulstrup J. Long-range protein electron transfer observed at the single-molecule level: In situ mapping of redox-gated tunneling resonance. PNAS 2005; 102(45) 16203-16208.

[51] Yagati A.K, Lee T, min J, Choi J.-W. A robust nanoscale biomemory device composed of recombinant azurin on hexagonally packed Au-nano array. Biosensors and Bioelectronics 2013; 40(1) 283-290.

[52] Artes, J.M, Diez-perez I, Sanz F, Gorostiza P. Direct measurement of electron transfer distance decay constants of single redox proteins by electrochemical tunneling spectroscopy. ACS Nano, 2011, 5 (3), 2060-2066.

[53] Alessandrini A, Corni S, Facci P. Unravelling single metalloprotein electron transfer by scanning probe techniques. Phys. Chem. Chem. Phys., 2006; 8, 4383-4397.

[54] Alessandrini A, Gerunda M, Canter, G.W, Verbeet, M.Ph., Facci, P. Electron tunnelling through azurin is mediated by the active site Cu ion. Chem. Phys. Lett., 2003; 376, 625-630.

[55] Kim S.U, Yagati A.K, Min J, Choi J.-W. Nanoscale protein-based memory device composed of recombinant azurin. Biomaterials 2010; 31(6) 1293-1298.

[56] Petrangolini P, Alessandrini A, Berti L, Facci P. An Electrochemical Scanning Tunneling Microscopy Study of 2-(6-Mercaptoalkyl)hydroquinone Molecules on Au(111). J. Am. Chem. Soc., 2010; 132, 7445-7453.

[57] Artes J.M, Lopez-Martinez M, Giraudet A, Diez-perz I, Sanz F, Gorostiza P. Current-voltage characteristics and transition voltage spectroscopy of individual redox proteins. J. Am. Chem. Soc., 2012, 134 (50), 20218-20221.

[58] Nagy G, Wandlowski T. Double Layer Properties of Au (111)/H2SO4 (Cl) + Cu^{2+} from Distance Tunneling Spectroscopy. Langmuir, 2003; 19, 10271-10280

[59] Wigginton, N.S, Rosso, K. M, Stack A.G. Hochella Jr, M.F. Long-Range Electron Transfer across Cytochrome−Hematite (α-Fe_2O_3) Interfaces. J. Phys. Chem. C, 2009; 113, 2096-2103.

[60] Kuznetsov A.M, Ulstrup J. Theory of electron transfer at electrified interfaces. Electrochimica Acta 2000; 45(15-16) 2339-2361.

[61] Pobolev I.V, Li Z, Wandlowski T. Electrolyte gating in redox-active tunneling junctions-An electrochemical STM approach. J. Am. Chem. Soc., 2008, 130 (47), 16045-16054.

[62] Mirkin M.V. Horrocks B.R Electroanalytical measurements using the scanning electrochemical microscope. Anal.Chim. Acta 2000; 406(2) 119-146.

[63] Wittstock G. Modification and characterization of artificially patterned enzymatically active surfaces by scanning electrochemical microscopy. Fresenius' Journal of Analytical Chemistry 2001; 370 (4) 303-315.

[64] Bollo S, Jara-Ulloa P. Finger S, Nunez-Vergara, L.J, Squella, J.A. Scanning electrochemical microscopy (SECM) study of superoxide generation and its reactivity with 1,4-dihydropyridines. J. Electroanal. Chem. 2005; 577, 235-242.

[65] Bauermann, L. P, Schuhmann, W, Schulte, A. An advanced biological scanning electrochemical microscope (Bio-SECM) for studying individual living cells. Phys. Chem. Chem. Phys., 2004; 6, 4003-4008.

[66] Macpherson J.V. Unwin P.R. Scanning electrochemical microscopy as an in vitro technique for measuring convective flow rates across dentine and the efficacy of surface blocking treatments. Electroanalysis 2005;17(3) 197-204.

[67] Wang, Y. Kececi, K. Velmurugan, J. Mirkin, M.V. Electron transfer/ion transfer mode of scanning electrochemical microscopy (SECM): a new tool for imaging and kinetic studies. Chem. Sci., 2013; 4, 3606-3616.

[68] Macpherson, J.V., Slevin, C.J., Unwin, P.R. Probing the oxidative etching kinetics of metals with the feedback mode of the scanning electrochemical microscope. J. Chem. Soc., Faraday Trans., 1996; 92, 3799-3805.

[69] Turcu F, Schulte A, Hartwich G, Schuhmann W. Imaging immobilised ssDNA and detecting DNA hybridisation by means of the repelling mode of scanning electrochemical microscopy (SECM). Biosensors and Bioelectronics 2004; 20(5) 925-932.

[70] Lu, X., Wang, Q., Liu, X. Review: Recent applications of scanning electrochemical microscopy to the study of charge transfer kinetics. Anal. Chim. Acta. 2007; 601, 10-25.

[71] Gonsalves M, Barker A L, Macpherson J V, Unwin P R, O'Hare D, Winlove C P. Scanning electrochemical microscopy as a local probe of oxygen permeability in cartilage. Biophys. J. 2000; 78(3) 1578-1588.

[72] Katemann B.B, Schulte A, Schuhmann W, Constant-Distance Mode Scanning Electrochemical Microscopy (SECM)—Part I: Adaptation of a Non-Optical Shear-Force-Based Positioning Mode for SECM Tips. Chem. Eur. J.,2003; 9: 2025-2033.

[73] nebel, M., Eckhard, K., Erichen T., Schulte, A., Schuhmann, W. 4D Shearforce-Based Constant-Distance Mode Scanning Electrochemical Microscopy. Anal. Chem., 2010, 82, 7842–7848.

[74] Treutler T.H, Wittstock G. Combination of an electrochemical tunneling microscope (ECSTM) and a scanning electrochemical microscope (SECM): application for tip-induced modification of self-assembled monolayers. Electrochimica Acta 2003; 48(20-22) 2923-2932.

[75] Lugstein, A., Bertagnolli, E., Kranz, C. Kueng, A., Mizaikoff, B. Integrating micro- and nanoelectrodes into atomic force microscopy cantilevers using focused ion beam techniques. Appl. Phys. Lett. 2002; 81, 349 (3pp).

[76] Katemann B.B, Schuhmann W. Fabrication and characterization of needle-type. Electroanalysis, 2002;14: 22-28.

[77] Kranz C, Friedbacher G, mizaikoff B. Integrating an ultramicroelectrode in an afm cantilever: combined technology for enhanced information. Anal. Chem., 2001; 73 (11) 2491-2500.

[78] Neufeld, A.K., O'Mullane, A.P. Effect of the mediator in feedback mode-based SECM interrogation of indium tin-oxide and boron-doped diamond electrodes. J Solid State Electrochem. 2006; 10, 808-816.

[79] Szamocki R, Velichko A, Holzapfel C, mucklich F, Ravaine S, Garrigue P, Sojic N, Hempelmann R, Kuhn A. Macroporous ultramicroelectrodes for improved electroanalytical measurements. Anal. Chem., 2007; 79(2), 533-539.

[80] Hermans A, Wightman M. Conical tungsten tips as substrates for the preparation of ultramicroelectrodes. Langmuir, 2006; 22 (25), 10348-10353.4

[81] Sachs C, Hildebrand M, Volkening S, Ertl G, Spatiotemporal self-organization in a surface reaction: from the atomic to the mesoscopic scale. Science 2001; 293 (5535) 1635-1638.

[82] Zamborini F.P, Crooks, R.M. In-situ electrochemical scanning tunneling microscopy (ECSTM) study of cyanide-induced corrosion of naked and hexadecyl mercaptan-passivated Au(111). Langmuir 1997; 13(2) 122-126.

[83] Papadantonakis, K.M., Brunschwig, B.S., Lewis, N.S. Use of Alkane Monolayer Templates To Modify the Structure of Alkyl Ether Monolayers on Highly Ordered Pyrolytic Graphite. Langmuir, 2008; 24, 857–861.

[84] Stieg A. Z, Rasool H. I, Gimzewski J.K. A flexible, highly stable electrochemical scanning probe microscope for nanoscale studies at the solid-liquid interface. Review of Scientific Instruments 2008; 79 (10) 103701-7.

[85] Stoll E, Marti O. Restoration of scanning-tunneling-microscope data blurred by limited resolution, and hampered by 1/f like noise. Surface science 1987; 181(1-2) 222-229.

[86] Eigler D.M, Schweizer E.K. Positioning single atoms with a scanning tunnelling microscope. Nature 1990; 344, 524-526.

[87] Reiss G, Bruckl H, Vancea J, Lecheler R, Hastreiter E. Scanning tunneling microscopy on rough surfaces-quantitative image analysis. J. Appl. Phys.1991; 70, 523-525.

[88] Endres, F., Borisenko, N., Abedin, S. Z. E., Hayes, R., Atkin, R. The interface ionic liquid(s)/electrode(s): In situ STM and AFM measurements Faraday Discuss., 2012; 154, 221-233.

[89] Atkin, R., Abedin, S. Z. E., Hayes, R., Gasparotto, L.H.s., Borisenko, N., Endres, F. AFM and STM Studies on the Surface Interaction of [BMP]TFSA and [EMIm]TFSA Ionic Liquids with Au(111). J. Phys. Chem. C, 2009, 113 (30), 13266–13272.

[90] Macpherson, J.V., Unwin, P.R., Combined Scanning Electrochemical−Atomic Force Microscopy. Anal. Chem., 2000, 72 (2), 276–285.

[91] Hai, N.T.M., Huynh, T.M.T., Fluegel, A., Mayer, D., Broekmann, P. Adsorption behavior of redox-active suppressor additives: Combined electrochemical and STM studies. Electrochimica Acta. 2011; 56, 7361-7370.

[92] Gewirth, A.A., Niece, B.K. Electrochemical Applications of in Situ Scanning Probe Microscopy, Chem. Rev. 1997; 97, 1129−1162.

IntechOpen